energies

MDPI

Article

Evaluation of Heated Window System to Enhance Indoor Thermal Comfort and Reduce Heating Demands Based on Simulation Analysis in South Korea

Hyomun Lee [1], Kyungwoo Lee [2], Eunho Kang [1], Dongsu Kim [1], Myunghwan Oh [3] and Jongho Yoon [1,*]

[1] Department of Architectural Engineering, Hanbat National University, Daejeon 34158, Republic of Korea
[2] Sustainable Design Team of R & D Center, Junglim Architecture, Seoul 04526, Republic of Korea
[3] Center for Climatic Environment Real-Scale Testing, Energy Division, Korea Conformity Laboratories, Seosan 31900, Republic of Korea
* Correspondence: jhyoon@hanbat.ac.kr

Abstract: Heated glass can be applied to improve windows' condensation resistance and indoor thermal comfort in buildings. Although this applied technology has advantages, there are still some concerns in practical applications, such as additional energy consumption and control issues. This study evaluates the effectiveness of a heated window heating (HWH) system in terms of thermal comfort and heating energy performance (HEP). The simulation-based analysis is performed to evaluate the effectiveness of the HWH using a residential building model and to compare it with radiant floor heating (RFH) and hybrid heating (HH) systems (i.e., combined HWH and RFH). This study also investigates the peak and cumulative heating loads using HWH systems with various scenarios of control methods and setpoint temperature. The predicted mean vote (PMV) is used as an indoor thermal comfort index. The ratio of cumulative thermal comfort time to the entire heating period is calculated. The results show that HWH and HH can reduce the heating load by up to 65.60% and 50.95%, respectively, compared to RFH. In addition, the times of thermal comfort can be increased by 12.55% and 6.98% with HWH and HH, respectively. However, considering the social practices of South Korea, HH is more suitable than HWH. Further investigations for HH show that a surface setpoint of 26 °C is proper, considering both heating demands and thermal comfort. In addition, the setpoint temperature should be determined considering HEP and the thermal comfort for HWH, and the optimal setpoint temperature was suggested under specific conditions.

Keywords: heated window heating; radiant floor heating; thermal comfort; predicted mean vote; control method

check for updates

Citation: Lee, H.; Lee, K.; Kang, E.; Kim, D.; Oh, M.; Yoon, J. Evaluation of Heated Window System to Enhance Indoor Thermal Comfort and Reduce Heating Demands Based on Simulation Analysis in South Korea. *Energies* **2023**, *16*, 1481. https://doi.org/10.3390/en16031481

Academic Editor: Paulo Santos

Received: 12 January 2023
Revised: 26 January 2023
Accepted: 30 January 2023
Published: 2 February 2023

Copyright: © 2023 by the authors. Licensee MDPI, Basel, Switzerland. This article is an open access article distributed under the terms and conditions of the Creative Commons Attribution (CC BY) license (https://creativecommons.org/licenses/by/4.0/).

1. Introduction

According to a 2022 UN report, approximately 34% of the global energy consumption in 2021 was attributed to buildings and construction, of which about 30% was consumed for heating, cooling, water heating, lighting, and cooking in buildings. In the buildings' part, 21% was consumed by residential buildings [1].

To improve the energy performance of buildings, the Republic of Korea has strengthened the thermal insulation performance of each part of the building. The country also implemented a zero-energy building certification system in 2020 to enhance the overall energy performance rather than that of specific building parts [2]. Currently, residential buildings in Seoul, Republic of Korea, must achieve a thermal insulation performance of at least 0.15 $W/m^2 \cdot K$ for exterior walls and 0.9 $W/m^2 \cdot K$ for windows. These performances are similar to the level for passive house standards (i.e., wall: 0.15 $W/m^2 \cdot K$, window: 0.8 $W/m^2 \cdot K$) [3]. Although the thermal insulation performance of windows has been substantially improved, they are still the thermally weakest part of the building envelope

when compared with the walls, roofs (0.15 W/m^2·K), and floors (0.15 W/m^2·K), which also constitute the envelope.

Windows with relatively poor thermal insulation degrade buildings' energy performance [4]. They also cause lower surface temperatures than the walls, roof, and floors, which negatively affects the thermal comfort of occupants owing to cold drafts [5]. Raising the heating setpoint to improve this situation increases energy consumption [6]. Moreover, low surface temperatures increase the probability of condensation on the window surface [7], obstructing the occupant's view of the outside [8].

One method to prevent condensation is to control the window's surface temperature to an appropriate level [4] by applying heated glass [9]. Heated glass is implemented by inserting a heating wire into the glass or using a transparent conductive coating layer on the glass surface [10]. When current is applied to the heated glass implemented with a heating wire or transparent conductive coating (TCC), heat is generated through electrical resistance. In architecture, the transparent conductive coating layer is widely used as opposed to heating wire insertion owing to its superior light transmittance and visibility, and research on this is actively underway.

Kurnitski et al. [9] investigated a method for estimating the efficiency and thermal transmittance of heated glazing by using the heat transfer theory. For typical glazing, the thermal transmittance can be determined as a single value under specific conditions depending on the glass, coating, air layer thickness, and composition of gas forming the air layer. However, for heated glazing, the thermal transmittance varies because different amounts of heat pass through the glazing depending on the temperature of the heated glass. Thus, researchers proposed a method for estimating the thermal transmittance and efficiency that reflects this feature. Lee et al. [10] experimentally measured the internal and external surface temperatures and heat flux of vacuum-heated glazing applied to residential buildings. These are measured by dividing to the center and edge of a large-area heated glazing. They also analyzed the heat gain and overheating tendencies based on measured data. The results were examined to identify the considerations for heated glass. They stressed that to prevent overheating, the temperature must be appropriately set depending on the purpose of the heated glass (condensation, comfort, heating, etc.) and to solve the difference in operating temperature between the center and the edge of a large-area heated glass. Cakó et al. [11] measured the thermal comfort of heated glass using two devices and analyzed the results according to the surface temperature and distance. In conditions where the metabolic rate is 1.0 MET, and the clothing insulation is 1.0 clo, the surface temperature of heated glass for thermal comfort is at least 40 °C. The authors stated that the required setpoint temperature for thermal comfort might vary with the experimental conditions (e.g., distance to an occupant, etc.), and stressed that thermal comfort is improved by using the heated glass. Lee et al. [12] used a simulation program to evaluate the heating energy performance of heated windows according to the improvements in the thermal insulation performance of building envelopes, such as the outer walls, floors, and windows in South Korea. They compared the performance with those of air-based heating and radiant floor heating and found that as the thermal insulation performance improved, the heating methods showed similar annual heating energy consumption. Based on these results, they noted the usefulness of heated glass for the heating system. To investigate the efficiency curves of heated glazing, Lee et al. [13] conducted both experimental and analytical studies to examine the heat fluxes under heating conditions of heated glass. Based on the results, they derived the efficiency curves according to the setpoint of the heated glass and the difference in air temperature between the internal and external. Moreau et al. [6] used an analytical method to evaluate the heating energy characteristics of heated windows. They found that the heating energy consumption was lower than required for typical double-glazed windows. They also emphasized that the effect was greater when the heated windows were installed on the east or west side than on the south side. Borys et al. [14] proposed a numerical analysis model based on the heat transfer for heated windows' indoor and outdoor heat flow and experimentally

validated the model. Krukovski et al. [15] performed an analytical method to evaluate the appropriate capacity for a heated window heating system in Ukraine. Mitsui and Sato [16] investigated the sheet resistance according to the materials and coating thickness used for the transparent conductive coating and experimentally derived the appropriate coating thicknesses of the materials.

The previous studies can be broadly divided into four categories. The first group of studies examined the sheet resistance of the transparent conductive coating layer, including the coating materials and thickness. The second group of studies researched the efficiency related to the internal and external heat flux of heated glazing. The subjects of the third and fourth groups are thermal comfort and the heating system as the research of architectural usefulness. Despite extensive research, few studies have comprehensively examined heating performance and thermal comfort for practical applications in buildings. Moreover, the perspectives of occupant comfort and energy use have not been adequately studied. To improve the thermal comfort of occupants close to the window, typically in the winter season [17], heating appliances underneath exterior windows are generally used. However, an inappropriate setpoint temperature of the heating appliances causes overheating [18], which is neither efficient for thermal comfort nor efficient for the energy consumption of buildings. It is necessary to evaluate the usefulness by comprehensively considering the thermal comfort and energy performance of heated windows.

Therefore, this study was conducted to comprehensively evaluate the usefulness of heated windows considering thermal comfort and energy performance. The evaluation was performed by modeling the living room of a residential building using a simulation program, and the region and weather conditions of Gangneung in South Korea. To evaluate the effectiveness of heated windows, the thermal comfort and energy performance were compared with the radiant floor heating. In this study, the usefulness of heated windows as a heating appliance was proven, and finally, a setpoint temperature was proposed by comprehensively considering thermal comfort and energy performance in the condition of this study.

2. Methodology

The effectiveness of the heated window system was evaluated by assessing heating loads and indoor thermal comfort behaviors based on the simulation-based analysis of residential zones. Three different heating systems (i.e., radiant floor heating, heated window heating, and hybrid heating systems) were considered to carry out the comparative analysis of each heating system. This section describes the features of the heated window system used in this study, details of the analysis model, and the evaluation method.

2.1. Properties of Heated Glass

Heated glass is implemented through three main methods. The first method involves inserting a nichrome heating wire into a typical glass, such as clear glass. This method is used in the rear windows of automobiles to ensure visibility by removing accumulated snow or frost. The second method involves attaching a heating film to the glass to generate heat [19], and the third method uses a TCC on a substrate. This method uses sputter-coating [12] or pyrolytic-coating to form TCC on the glass. The heated glass used in this study is manufactured using a atmospheric pressure chemical vapor deposition (AP-CVD) during glass manufacture. [20]. In the heated glass, glass is used as the substrate and is coated with a transparent conductive oxide to form the TCC layer. Suitable materials include indium tin oxide and fluorine-doped tin oxide (FTO). The heated glass used in this study was coated with FTO [20].

Figure 1 shows the transmittance and reflectance of heated glass [21] according to the wavelength measured with a solar spectrometer [22]. In the solar spectrometer, tungsten-halogen and deuterium lamps are used as a light source to measure reflectance and transmittance according to the wavelength. Table 1 shows the optical properties of the heated glass, calculated according to ISO 9050 [23] and KS L 2514 [24] based on the measurements

in Figure 1. Light transmittance and reflectance were calculated using the measured transmittance and reflectance by the solar spectrometer and the daylight spectrum as D_{65} [25], provided by the International Commission on Illumination. As a result, the ratio of the total transmitted energy or the total reflected energy to the total energy of D_{65} becomes the visible light reflectance or visible light transmittance. The other optical properties were calculated using transmittance and reflectance of the solar spectrometer and weighting factors for each wavelength. The heated glass showed high light transmittance of 82.5%, whereas the emissivity of the coated side was 0.16, approximately 20% that of the glass side. The results in Table 1 were input to the simulation program. The heated window was composed by assembling one heated glass and two low-emissivity glasses in the simulation program.

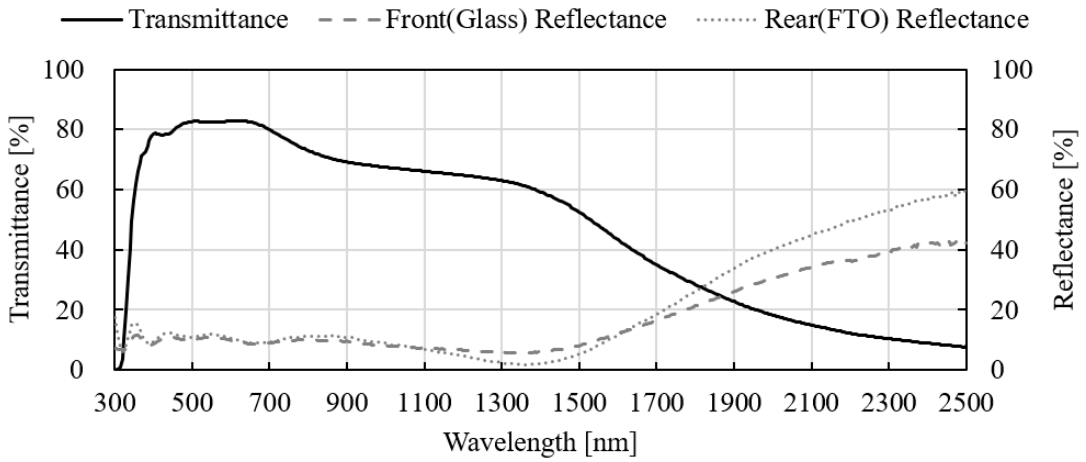

Figure 1. Transmittance and reflectance of heated glass at various wavelengths.

Table 1. Optical properties of heated glass.

Light Transmittance (%)	Light Reflectance (%)		Total Solar Transmittance (%)	Total Solar Reflectance (%)		UV Transmittance (%)	Emissivity (-)	
	Glass Side	FTO Side		Glass Side	FTO Side		Glass Side	FTO Side
82.5	10.4	11.3	69.7	10.6	11.6	52.5	0.84	0.16

2.2. Simulation Model for Analysis of Heating Load and Thermal Comfort

This study used ESR-r (i.e., Environmental System Performance-reference) [26], a dynamic simulation program for assessing building energy, to analyze the heating load and thermal comfort when a heated window was used for heating supply. A feature of ESP-r that defines the heating at a specific node was used to evaluate the application of heated glass to heating. Figure 2 shows the building model and the cross-section of the heated glazing in ESP-r. In Figure 2b, the thick lines represent the low-e coating and TCC, and the dots are the nodes that can be defined as the heating surface of the window in ESP-r. The red node is the heating surface of the model in this study. Since this method of modeling heated windows in EPS-r has already been used and validated in a previous study [13], an additional verification process was not performed in this study.

The building simulation model for the analysis included three zones: the glass zone located on the southernmost side, followed by the room zone and the common zone. There was no physical zone division between the glass zone and the room zone. Since the analysis program does not allow the use of multiple heating systems in a zone, this study assumed the zone (i.e., the domestic area) was divided into two zones, including room and glass zones. The building was modeled with the size of a living room in a 100 m^2 apartment house, the standard housing area in the laws for a place in South Korea [27]. The floor area of the building model, excluding the common zone, was 24 m^2, the window area on the south side was 9.6 m^2, and the window-to-floor ratio was 40%.

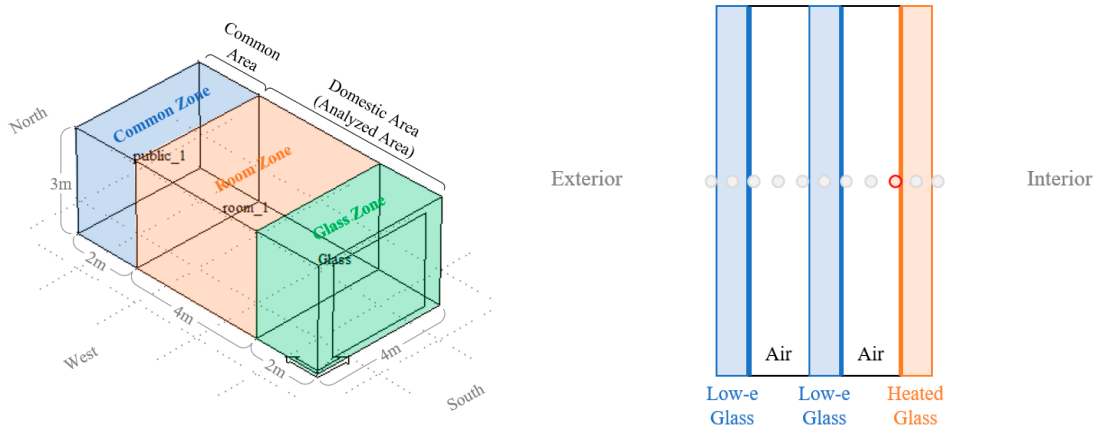

Figure 2. Illustration of the model and heated glazing in the simulation program. (**a**) The building model in the simulation program; (**b**) The section layout of heated glazing.

The boundary conditions for the analysis model's side walls (east-facing and west-facing walls) were modeled under the adiabatic with no heat flow, assuming they are in contact with the adjacent households. The boundary condition for the north wall of the room zone was modeled to be in touch with common spaces (corridors, stairwells, etc.), thus creating a heat flow even though it was not directly exposed to the outdoor air. Two models with different floor boundary conditions were generated to evaluate the effect of heat loss through the ground. Model 01 used a boundary condition that assumed contact with the ground. Model 02 used the adiabatic boundary condition with no heat flow between households, assuming the household was located on an intermediate story. The thermal insulation performance of each component (i.e., walls, roofs, floors, etc.) was modeled to meet Korean regulations. The thermal transmittance of typical windows and windows with heated glass was identically defined. Since the optical properties of heated windows differ from those of typical windows, a heating function was added. Table 2 summarizes the main aspects of the analysis model.

Table 2. Details of the simulation model.

Category and Items		Model 01 (Ground Floor)			Model 02 (Typical Floor)		
Floor area (m^2)		24					
Window area (m^2)		96					
Window-to-floor ratio (%)		40					
Thermal transmittance ($W/m^2 \cdot K$)	Exterior wall	0.129					
	Interior wall	0.184					
	Window	0.721					
	Heated window	0.721					
	Between floors	-			0.782		
	Ground floor	0.147			-		
Boundary condition	Zone	Glass	Room	Common	Glass	Room	Common
	Roof (ceiling)	Similar current			Adiabatic		
	Wall (east, west)	Adiabatic		Exterior	Adiabatic		Exterior
	Wall (south)	Exterior	Zone (Glass)	Zone (Room)	Exterior	Zone (Glass)	Zone (Room)
	Wall (north)	Zone (Room)	Zone (Common)	Exterior	Zone (Room)	Zone (Common)	Exterior
	Floor	Ground			Adiabatic		

To focus the evaluation on the effect of applying the heated glass to heating, internal heat gain elements such as occupants, lighting, and devices were not modeled. The heating setpoint was set to 22 °C, and the heating systems worked to control the indoor air temperature. The heating device capacity of each system was determined based on auto-sized values automatically calculated with the design-day condition. Radiant floor heating and heated window heating were applied to analyze the performance variations between the two methods. Table 3 and Figure 3 show each heating method's heat source locations and indoor air-temperature sensor locations.

Table 3. Sensor, actuator, and setpoint of each heating system.

	Radiant Floor	**Heated Window**	**Hybrid 01**	
			Radiant Floor	**Heated Window**
Sensor	Dry bulb temperature	Dry bulb temperature	Dry bulb temperature	Dry bulb temperature
Sensor location	Room zone	Glass zone	Room zone	Glass zone
Actuator	Room zone	Glass zone	Room zone	Glass zone
Setpoint (°C)	22			
Heating period	January to March, September to December			

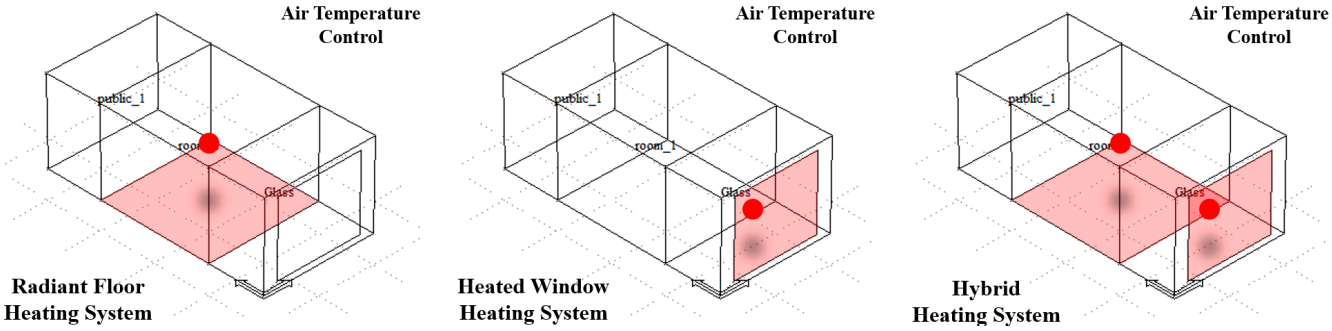

Figure 3. Heating surface and air temperature sensing point of each heating system.

The weather data for the Gangneung region in South Korea were used to investigate the heating load and thermal comfort, which were included in the simulation tool. The data from the International Weather for Energy Calculations 1.1, created and provided by the American Society of Heating, Refrigerating, and Air-conditioning Engineers (ASHRAE), were used as the weather data. Table 4 presents the monthly characteristics of each meteorological item. Since the ground temperature was not included in these meteorological data, the ground temperature was defined based on the average ground temperature from 1981 to 2010, which was provided by the Korea Meteorological Administration [28].

Figure 4 depicts the location and climate classification of Gangneung, South Korea, using the Koppen–Geiger climate classification map [29]. The climate classification of South Korea, including Gangneung, belongs to the humid continental climate. The northern states of the United States, and the border area between Europe and Russia, show the same climatic characteristics.

Table 4. Weather data used in the simulation model.

Month	Dry Bulb Temperature (°C)			Relative Humidity (%)	Wind Speed (m/s)	Ground Temperature (Depth: 1.5 m) (°C)
	Avg	Max	Min			
January	0.4	10.7	−9.8	46.8	3.0	9.1
February	2.2	13.6	−8.5	56.6	2.6	7.1
March	5.6	15.4	−3.5	54.4	2.7	7.2
April	12.4	27.0	1.7	58.6	2.9	9.3
May	18.0	34.0	6.9	62.5	2.7	12.6
June	20.6	29.9	14.3	73.9	1.6	16.0
July	24.0	34.1	17.2	77.4	2.2	19.3
August	24.9	37.1	16.5	78.3	1.5	21.7
September	20.1	28.5	14.2	72.9	1.9	22.0
October	15.2	25.7	5.3	66.6	2.3	19.9
November	9.0	19.6	−4.8	54.6	3.1	16.5
December	3.1	12.1	−6.2	50.6	3.3	12.6

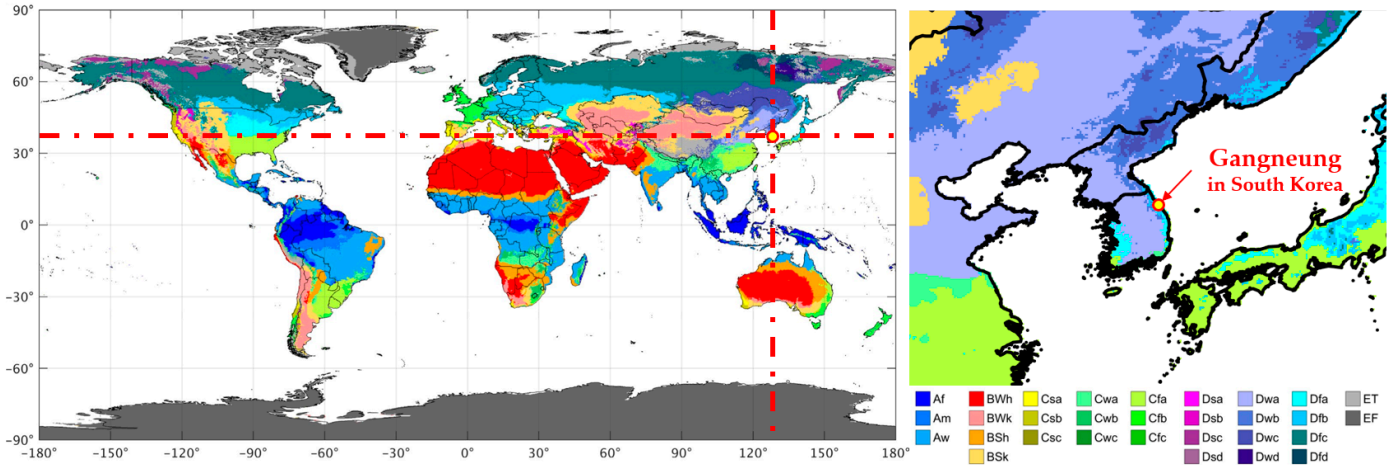

Figure 4. Location and climate classification of Gangneung in the Koppen–Geiger climate classification map [29].

2.3. Description of Indoor Thermal Comfort

The predicted mean vote (PMV), the thermal comfort index used in this study, was proposed in an experimental study by Fanger at the Technical University of Denmark. It expresses the average thermal sensation experienced by people in a given environment [30]. The PMV can be used as an index to evaluate the comfort level of indoor environments in residential buildings, offices, hospitals, etc., and to control the heating and cooling facilities. It has been introduced as a thermal comfort index in ISO 7730 [31] and ASHRAE 55 [32], which are international standards. PMV is calculated by considering the heat transfer between the body and surrounding environment using two parameters of the occupant (i.e., metabolic rate and insulating of clothing) and four parameters of the indoor environment (i.e., air temperature, mean radiant temperature (MRT), air velocity, and humidity). Additionally, as shown in Table 5, PMV is calculated as a value ranging from +3 to −3, which is the range of thermal sensation from hot to cold. Values closer to −3 indicate a thermal comfort level where the occupants feel colder, whereas values closer to +3 indicate an environment where occupants feel hotter. Hence, a PMV of 0 represents the optimal comfort level; statistically, 95% of the occupants are satisfied with the indoor

environment. ISO 7730 [31] and ASHRAE 55 [32] recommend a PMV range of −0.5 to 0.5 to provide indoor comfort.

Table 5. Seven-point thermal sensation scale.

Hot	Warm	Slightly Warm	Neutral	Slightly Cool	Cool	Cold
+3	+2	+1	0	−1	−2	−3

The input variables were set to evaluate the thermal comfort according to each heating method, as shown in Table 6. The input meteorological data and model characteristics were reflected to calculate the air temperature, relative humidity, and MRT in the analysis program. In addition, the air velocity, metabolic rate, and insulation of clothing values were direct inputs into the simulation program. A value of 0.1 m/s was input for the air velocity considering the indoor conditions, whereas those for metabolic rate and clothing insulation were 1.5 MET and 0.7 clo, respectively. According to ISO 7730, insulation of clothing of 0.7 clo signifies wearing undergarments, shirts, trousers, socks, and shoes, and a metabolic rate of 1.5 MET designates standing and light activity (shopping, laboratory work, light industry). The PMV of the glass zone and room zone were calculated every hour using the analysis program, based on which the cumulative hours in each PMV range were analyzed to evaluate thermal comfort behaviors.

Table 6. Input values to calculate the PMV.

Air Temperature (°C)	Relative Humidity (%)	Mean Radiant Temperature (°C)	Air Velocity (m/s)	Metabolic Rate (-)	Cloth (-)
Value calculated by the simulation model			0.1	1.5	0.7

3. Heating Load and Thermal Comfort of Heating Systems

3.1. Heating Load Comparison for Each Heating System

As shown in Figure 3, in radiant floor heating, the room zone and glass zone are heated via room zone heating, whereas in heated window heating, they are heated via glass zone heating. Therefore, the indoor air temperature may differ between the heating zone and adjacent zones, and the accuracy of the analysis model used in this study will deteriorate if the temperature difference is large.

Figure 5 shows each model's indoor air temperatures of the glass zone and room zone according to the floor boundary condition and heating system. The top graph presents the indoor air temperature over time for each model, and the scatter plots below this present the indoor temperature distribution of the room zone to the glass zone for each model. According to the graphs of radiant floor heating and hybrid heating, the air temperature of the room zone with respect to the glass zone was controlled at a low level. The times were observed in which the air temperature of the glass zone was high owing to daytime solar radiation, which caused a difference in the air temperature between the two zones. Since these times are different from the times needed for heating in the model, it is expected to have no substantial impact on the results of this study.

Figure 6 presents the heating load concerning the outdoor air temperature for each heating method. The load is depicted only for outdoor air temperatures lower than the heating setpoint (22 °C). In Figure 6a, the floor boundary condition is the ground, whereas Figure 6b shows the adiabatic, which relates to the floor between two stories. Radiant floor heating showed the highest peak heating load under both floor boundary conditions, followed by hybrid heating and window heating. Table 7 presents the peak heating load of each heating method.

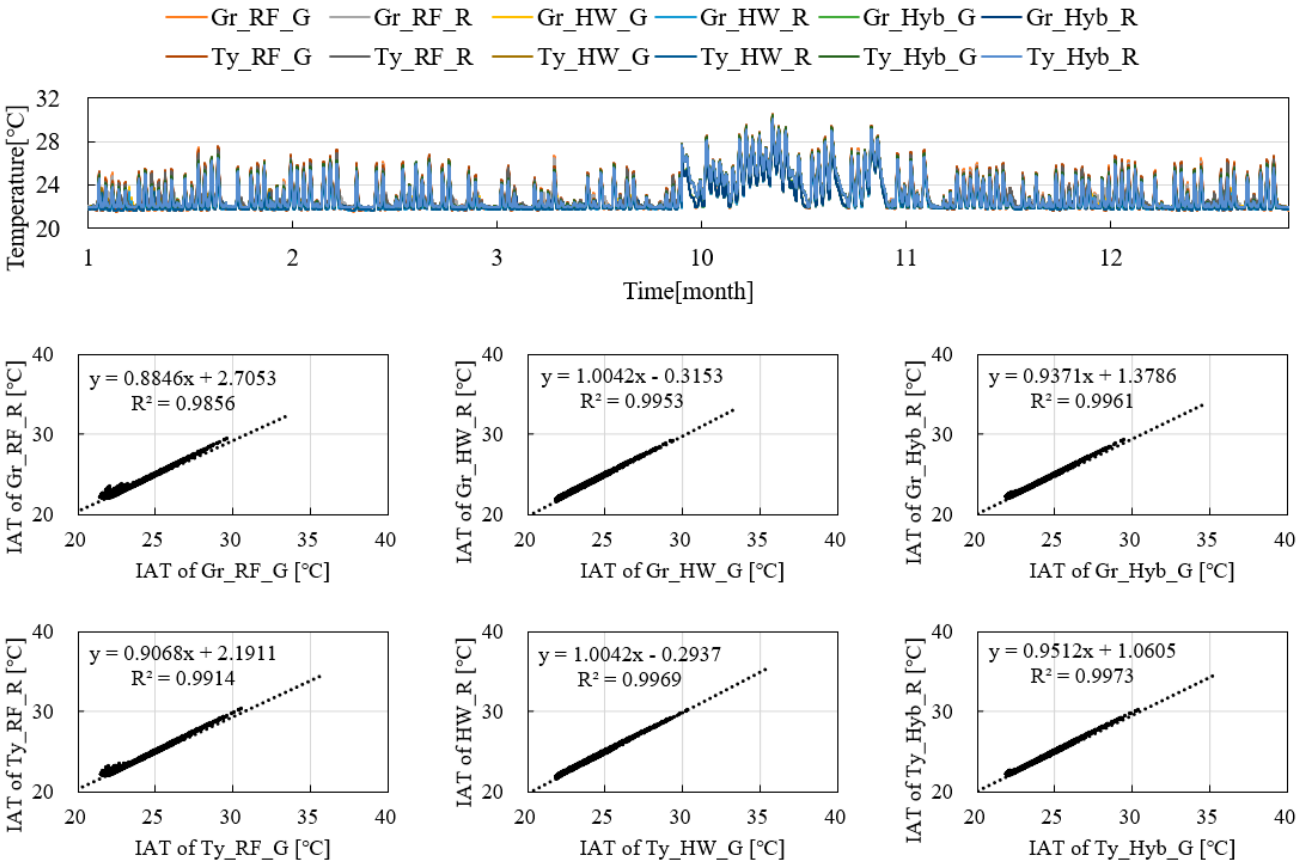

Figure 5. Outdoor air temperature (OAT) and indoor air temperature (IAT) of the glass zone (G) and room zone (R) of simulation models according to the floor boundary condition (ground floor: Gr, typical floor: Ty) and heating system.

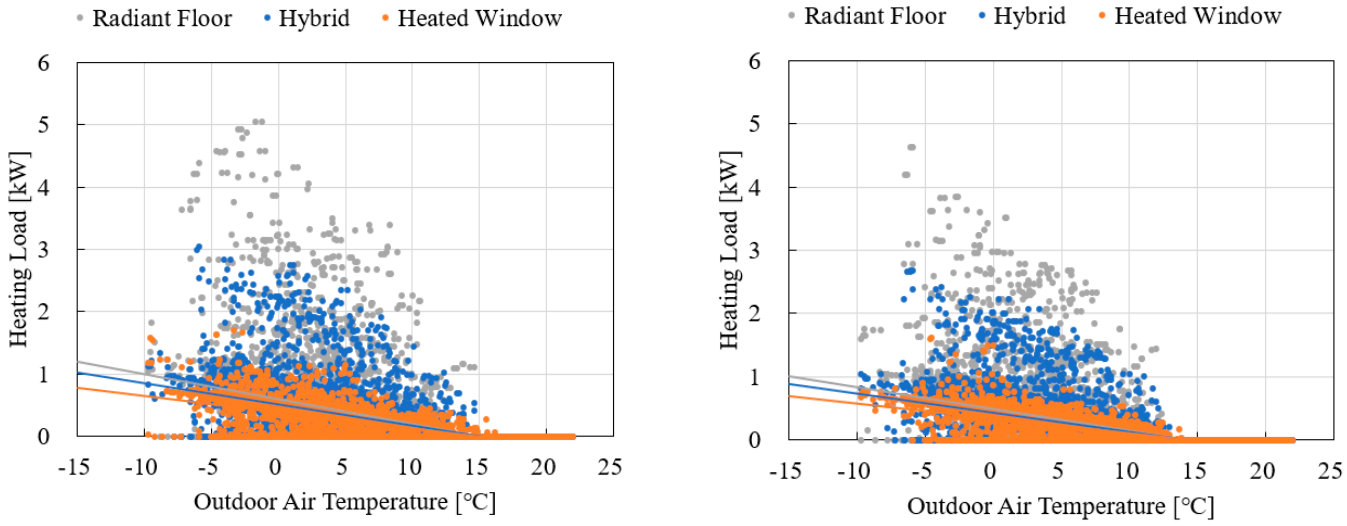

(**a**) (**b**)

Figure 6. Variation in heating load with outdoor air temperature for each simulation model. (**a**) Ground floor; (**b**) Typical floor.

Table 7. Peak heating load and cumulative heating load of each simulation model.

Boundary Condition		Ground Floor				Typical Floor			
Heating System		Radiant Floor	Heated Window	Hybrid		Radiant Floor	Heated Window	Hybrid	
				Radiant Floor	Heated Window			Radiant Floor	Heated Window
Peak Load (kW)		5.04	1.70	2.47	0.85	4.62	1.62	2.21	0.95
Cumulative heating load (kWh)	January	395.78	266.83	231.45	114.81	327.78	233.5	186.11	103.65
	February	318.90	213.66	188.58	92.51	249.03	178.34	144.24	78.27
	March	327.06	223.02	196.55	92.09	253.96	184.14	152.17	76.98
	April	-	-	-	-	-	-	-	-
	May	-	-	-	-	-	-	-	-
	June	-	-	-	-	-	-	-	-
	July	-	-	-	-	-	-	-	-
	August	-	-	-	-	-	-	-	-
	September	-	-	-	-	-	-	-	-
	October	23.62	11.93	12.68	5.5	5.37	2.62	2.88	1.59
	November	188.52	122.17	109.82	53.91	147.83	97.11	85.8	40.15
	December	320.15	210.05	192.31	86.92	259.03	180.78	156.09	74.03
	Annual	1574.03	1047.66	931.39	445.74	1242.99	876.49	727.29	374.67

Compared with the ground floor model (ground floor boundary condition), the peak heating load of the typical floor model (adiabatic floor boundary condition) was small. Under radiant floor heating, heated window heating, and hybrid heating, the peak heating load was reduced by approximately 8.33%, 4.71%, and 12.17%, respectively. This trend is because the typical floor model has no heat loss through the floor.

The peak heating load ratio of each heating model to the radiant floor heating model was analyzed among the same boundary conditions of the floor. First, for the model with the ground floor, the peak heating load ratio relative to radiant floor heating was 33.73% for heated window heating and 60.32% for hybrid heating, whereas for the model with the typical floor, the ratios were 35.06% and 57.79%, respectively.

Table 7 presents each model's peak heating load and monthly and annual cumulative heating loads. The incremental heating loads exhibited the same trend observed in the above peak heating load analysis. Compared with the ground floor results, the typical floor showed small monthly and annual cumulative heating loads, and window and hybrid heating showed lower cumulative heating loads than radiant floor heating. However, compared with the reduction in the peak heating load by applying heated windows, the reduction in the cumulative heating load was small. For the ground floor model, the annual cumulative heating load ratio relative to radiant floor heating was 66.56% for heated window heating and 87.49% for hybrid heating, whereas the ratios were 70.51% and 88.65%, respectively, for the typical model.

According to the above analysis, the peak and cumulative heating loads were reduced when heated window heating was applied. This was because heating is provided via the heated window, which has the lowest thermal insulation performance (0.721 W/m^2) among the envelope components where heat is exchanged with the outdoor air or a common zone. The inner surface temperature of the heated window on heating is higher than the outdoor air and indoor temperatures, thus preventing heat loss through the window and reducing the heating load. Figure 7 shows the window's outdoor air temperature, indoor air temperature, and inner surface temperature in December for radiant floor heating and heated window heating in the typical floor model. As explained, under heated

window heating, the window's inner surface temperature was higher than the indoor air temperature. In contrast, under radiant floor heating, the window's inner surface temperature was lower than the indoor air temperature at night but higher during the daytime. This trend was also observed in the ground floor model.

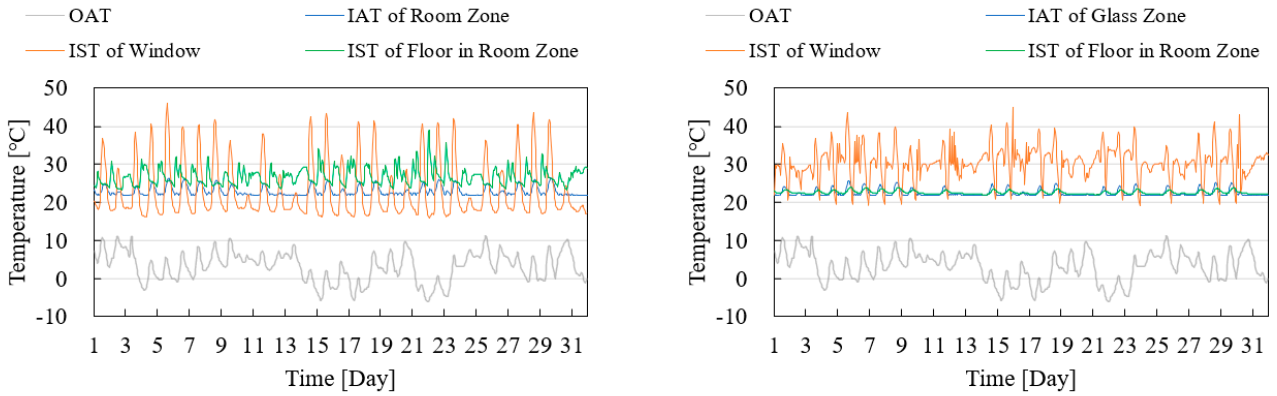

Figure 7. Outdoor air temperature (OAT), indoor air temperature (IAT), and interior surface temperature (IST) of window and floor for the ground floor model. (**a**) Radiant floor heating system; (**b**) Heated window heating system.

Under hybrid heating, the peak and cumulative heating loads were lower than those of radiant floor heating, although the heating load was higher than in heated window heating. The annual cumulative heating load was 31.9% and 25.8% higher than in heated window heating for the ground floor and typical floor, respectively. Figure 8 shows the analysis results for the typical floor. Figure 7a shows the cumulative heat fluxes for the window, south wall (glass zone), and north wall (room zone) of each model at night (00:00–04:00), that is, without the influence of solar radiation. Positive values indicate heat gain, whereas negative values indicate heat loss. Figure 7b shows the difference in indoor air temperature between each model's room zone and common zone for one week in December.

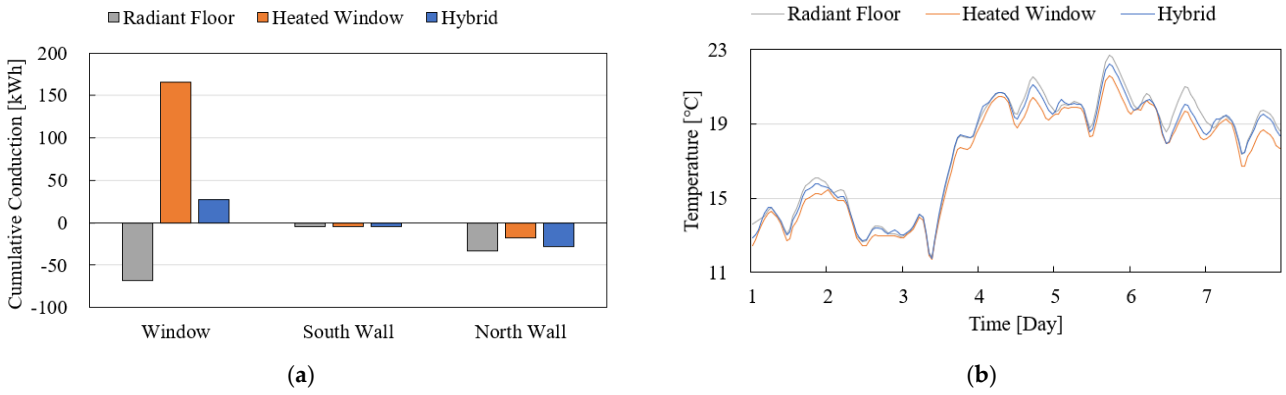

Figure 8. Inner surface conduction and difference in air temperature between room and common zones. (**a**) Cumulative conduction on inner surfaces of window, south wall (glass zone), and north wall (room zone) for each heating system at night (00:00–04:00); (**b**) Difference in air temperature between room zone and common zone for each heating system for one week (1–7 December).

According to Figure 7a, the heat fluxes of the window varied with the heating method, whereas the heat flux of the south wall did not greatly vary with the heating method. However, the heat flux of the north wall greatly varied with the heating method. As the thermal transmittance and boundary condition of the north wall were identical for each model, they should not differ according to the heating method; however, this study

observed a difference. As shown in Figure 3, the temperature sensor and heating surface location varied for each model according to the heating method. In the hybrid heating model, because temperature sensing and heating were applied in the room zone and glass zone, the air temperature of the room zone was formed according to the setpoint of 22 °C.

Conversely, in the heated window heating model, temperature sensing and heating were applied to the glass zone; hence, the glass zone and room zone had similar air temperatures, whereas the air temperature in the room zone was a little lower than 22 °C. This caused a difference in the air temperature variation and, consequently, a heat flux difference between the room zone and the common zone for each model. Figure 7b shows the air temperature difference between each model's room zone and common zone, which was larger in the hybrid heating model than in the heated window heating model.

3.2. Thermal Comfort Comparison for Each Heating System

Figure 9 and Table 8 show the ratio according to each PMV range for each model over the entire analysis period. The glass zone and room zone results for each model under both floor boundary conditions are presented. Since heating was applied, the PMV was never lower than −0.5 and was occasionally higher than 1.0. The hours when the PMV was outside the thermal comfort range and evaluated as "warm" or "hot" were attributed to irradiance during the daytime.

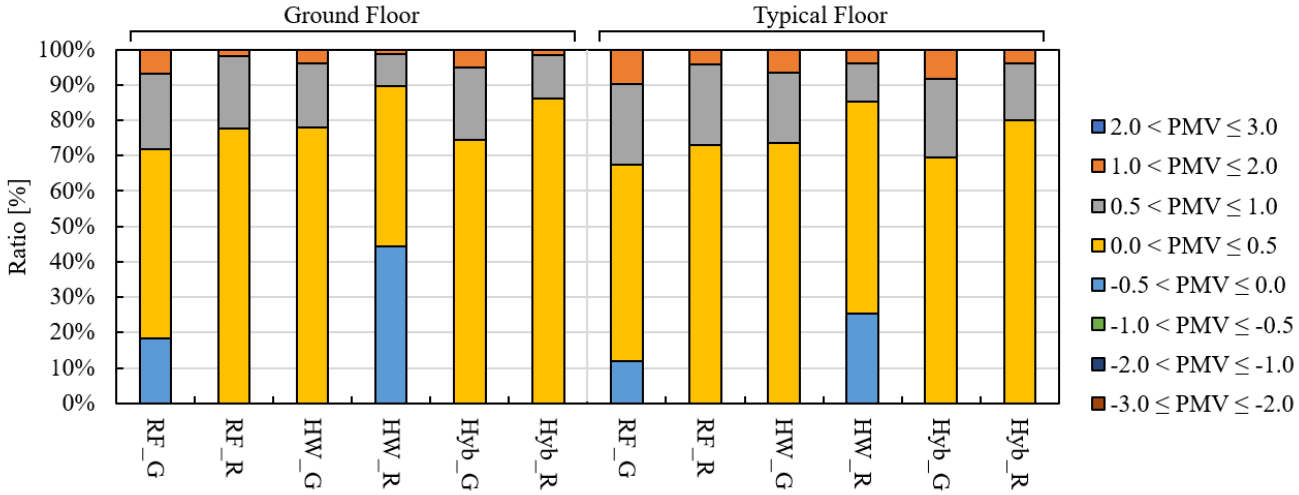

Figure 9. Ratio of comfort time for each model.

Table 8. Cumulative hours for various ranges of PMV and comfort ratio (−0.5 ≤ PMV ≤ 0.5).

PMV Range	Ground Floor						Typical Floor					
	Radiant Floor		Heated Window		Hybrid		Radiant Floor		Heated Window		Hybrid	
	G	R	G	R	G	R	G	R	G	R	G	R
2.0 < PMV ≤ 3.0	-	-	-	-	-	-	2	-	2	-	2	-
1.0 < PMV ≤ 2.0	293	80	171	60	227	70	426	179	286	170	359	177
0.5 < PMV ≤ 1.0	934	897	793	392	891	534	1000	1003	8872	479	971	699
0.0 < PMV ≤ 0.5	2336	3391	3403	1984	3247	3764	2423	3186	3208	2605	3036	3492
−0.5 < PMV ≤ 0.0	805	-	1	1932	3	-	517	-	-	1114	-	-
Comfort Ratio	71.91	77.63	77.93	89.65	74.40	86.19	67.31	72.94	73.44	85.14	69.51	79.95

First, differences were observed in the PMV according to the floor boundary condition. Compared with the ground floor, the ratio of time that PMV was lower than 0 was higher on the specific model with the typical floor because heat loss through the floor did not occur during heating. Additionally, the ratio of time that PMV was higher than 0.5 was

higher in all models with the typical floor because heat loss through the floor did not occur under overheating caused by irradiance.

Heated window heating and hybrid heating exhibited better thermal comfort than radiant floor heating. According to the PMV analysis results for the typical floor, 70.12% (glass zone: 67.31%, room zone: 72.94%) of the total 4368 h of radiant floor heating was in the thermal comfort range in terms of the PMV. Under heated window heating and hybrid heating, 79.29% (glass zone: 73.44%, room zone: 85.14%) and 74.73% (glass zone: 69.51%, room zone: 79.95%) were in the thermal comfort range, respectively. Hence, the heating methods, including heated windows, were more advantageous than radiant floor heating in terms of thermal comfort.

For the typical ground condition, the ratio of time of thermal comfort according to the heating method was compared based on the room zone. The ratio showed that heated window heating and hybrid heating were approximately 16.73% and 9.60% higher than radiant floor heating. This indicates that heated window heating improves the occupants' thermal comfort.

Among the factors determining the PMV, the MRT can be influential depending on the heating method. Except for radiant floor heating, other heating methods have heated window heating; therefore, when heat is generated from windows with low surface temperatures in winter, relatively high window surface temperatures are formed. This results in a higher MRT than that achieved in radiant floor heating. Figure 10 presents the MRT of the glass zone for each model under the typical floor condition from 1 to 14 December. The MRT in the daytime was increased because of irradiance. At night, when there is no influence of irradiance, the MRT varied with the heating device, and it was approximately 22.5 °C under radiant floor heating and about 24 °C under heated window heating, which is a difference of roughly 1.5 °C. The MRT of hybrid heating was also below that of heated window heating, although it was higher than that of radiant floor heating.

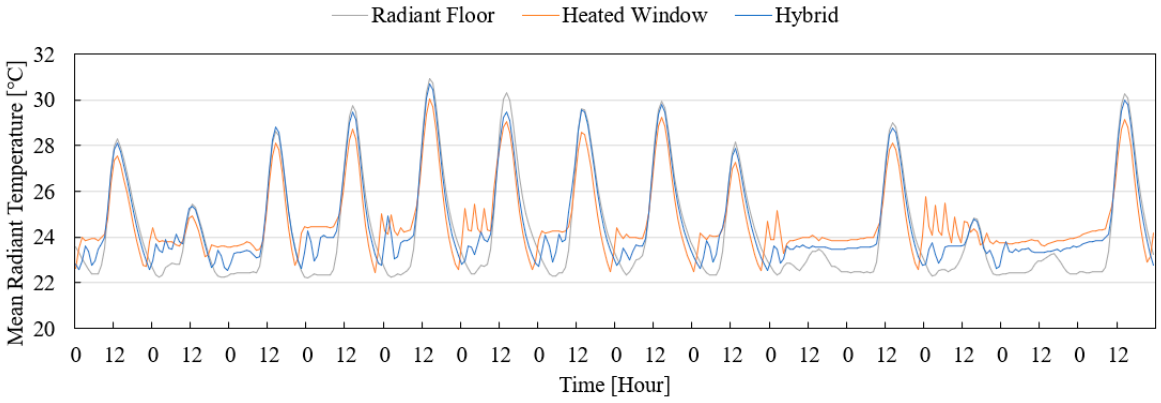

Figure 10. Mean radiant temperature of the glass zone of each model under the typical floor condition.

Radiant floor heating is the traditional and typical heating method for residential buildings in South Korea. This is related to the Korean custom of not wearing shoes in residential spaces. Hence, the floor surface temperature is a major factor determining the occupants' thermal comfort. Figure 11 shows the floor surface temperature of the room zone for the period of 1–7 December for each model. Under heated window heating, the floor surface temperature was distributed from approximately 22 to 23 °C. In contrast, the surface temperature was higher than 25 °C during the heating period under radiant floor heating and hybrid heating. In the area shaded in red, the temperature difference between heated window heating and hybrid heating was approximately 5 °C, which is greater than that with radiant floor heating.

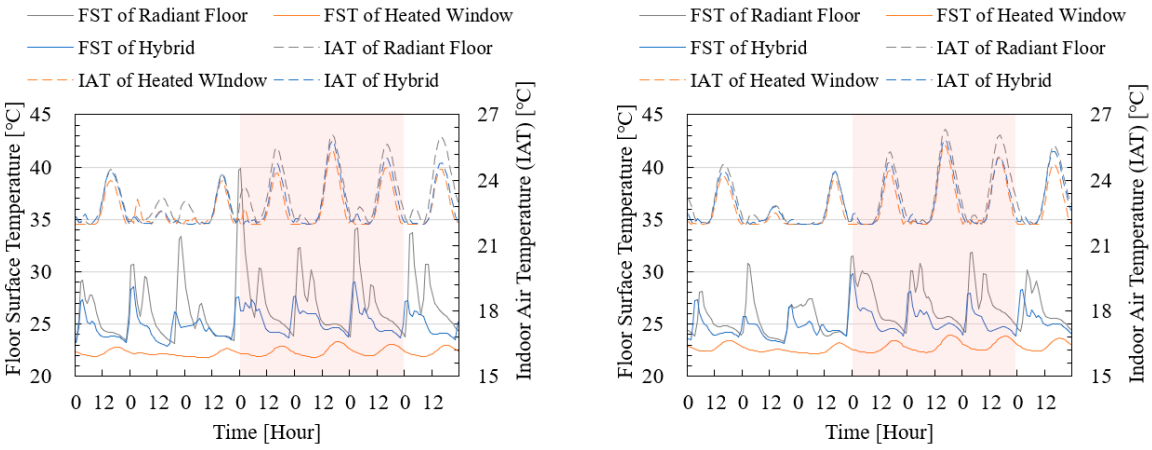

Figure 11. Each model's floor surface temperature (FST) and the indoor air temperature (IAT) of each model. (**a**) Ground Floor; (**b**) Typical Floor.

Considering the results of the heating load and thermal comfort from the previous analysis, heated window heating appears to be the most appropriate heating method. However, as explained above, the floor surface temperature is important in Korea. In a previous study [2] that applied a low-temperature radiant floor heating system using an air-source heat pump, the indoor air setpoint was set to 26–28 °C to increase the floor surface temperature. Therefore, hybrid heating combining heated window heating with radiant floor heating is considered suitable for such a case.

4. Comparative Study Based on Control Method of the Hybrid Heating System

The heating load and thermal comfort according to the control method of hybrid heating, which combines radiant floor heating with heated window heating, were evaluated. Figure 12 shows the models of two hybrid heating systems. Figure 12a shows the air-temperature sensing model for heated window systems in the hybrid heating system. It is the same hybrid heating system as that used in Section 3. Figure 12b shows the model of surface-temperature sensing for the hybrid heating system's heated window heating system. The difference between the two models is only the temperature sensing location to control the heated window heating system. In addition to the temperature sensing location for controlling the operation of the heated window, the setpoint for controlling the surface-temperature sensing was changed from 22 to 36 °C, and the heating load and thermal comfort characteristics were comparatively analyzed. The floor boundary condition applied here was the same as that of the typical floor.

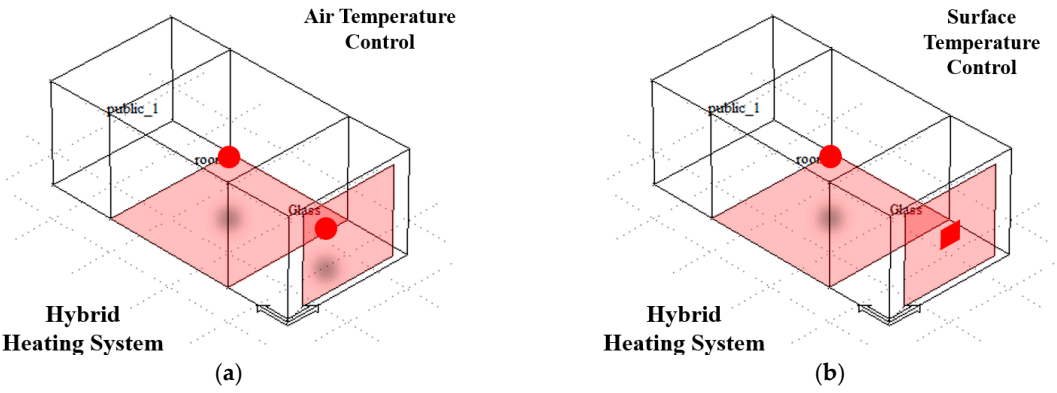

Figure 12. Heating surface and temperature sensing point of hybrid heating systems. (**a**) Air-temperature sensing model; (**b**) Surface-temperature sensing model.

4.1. Heating Load Comparison According to Control Method and Setpoint

Figure 13 shows the variation in the heating load under hybrid heating according to the control method of the heated window and the setpoint. "Air" indicates the air temperature control method, as in Figure 12a, and "Sur" indicates the surface temperature control method, as in Figure 12b. First, the hybrid heating model using the air temperature control method with a setpoint of 22 °C showed an annual cumulative heating load of 1101.96 kWh. When the temperature sensing location was changed to the glass surface while maintaining the setpoint, the annual cumulative heating load increased by approximately 6.60% to 1174.65 kWh. The annual cumulative heating load changed as the setpoint of the heated window surface increased, with the lowest cumulative heating load observed at a setpoint of 30 °C. The annual cumulative heating load was 1063.17 kWh, approximately 5.52% lower than that in the air temperature control model and 9.49% lower than that in the surface temperature control model with a setpoint of 22 °C. The load tended to increase at setpoints higher than 30 °C.

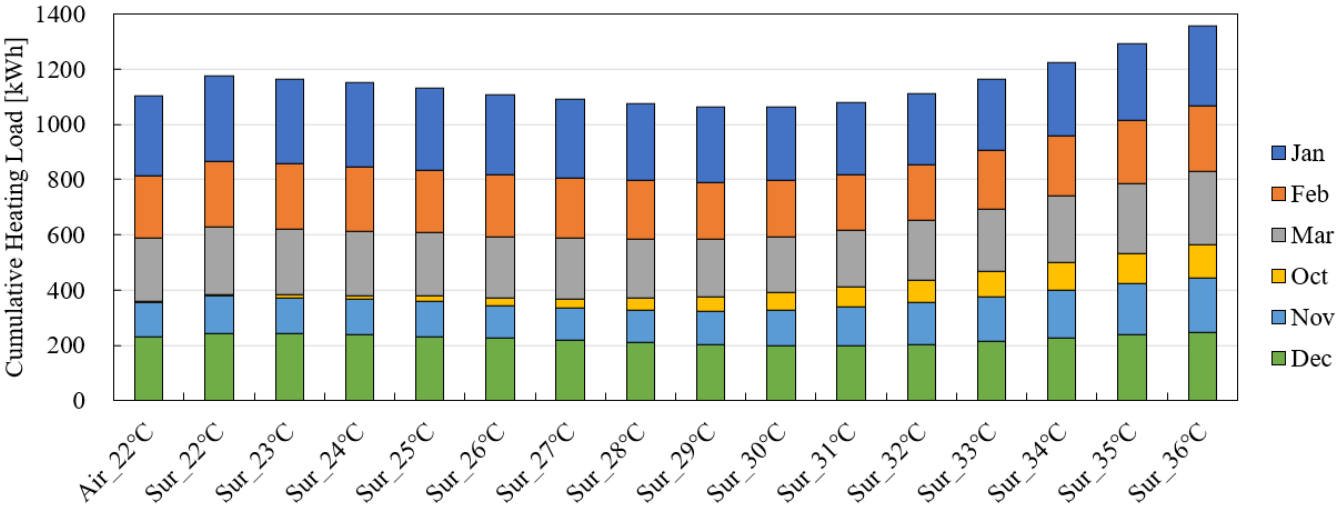

Figure 13. Variation in monthly heating load according to the control method and setpoint.

Figure 14 shows the ratio of the monthly heating load to the annual cumulative heating load of each model. By month, from January to March and October to December, the hybrid heating model using air temperature control with a setpoint of 22 °C showed ratios of 26.29%, 20.19%, 20.79%, 0.41%, 11.43%, and 20.88%, respectively. The total annual cumulative heating load increased when the temperature sensing location was changed to the glass surface while maintaining the setpoint. However, there was no significant difference in the ratio. As the setpoint of the surface temperature control method increased, the monthly ratio changed; in January, February, and December, it tended to decrease as the setpoint increased. In contrast, as the setpoint increased in October, the ratio continuously increased from 0.61% to 8.93%. In March and November, it tended to increase after showing the lowest ratio at a specific setpoint. In March, the annual cumulative heating load was approximately 19.12% at the lowest setpoint of 30 °C; in November, it was about 10.70% at 27 °C.

Figure 15 shows the ratio of the heating load to the annual cumulative heating load of each heating system for each model. First, in the air temperature control model with a setpoint of 22 °C, radiant floor heating showed a ratio of approximately 66.0%, whereas that for heated window heating was about 34.0%. In the surface temperature control model with the same setpoint, radiant floor heating and heated window heating showed ratios of 82.94% and 17.06%, respectively. As the heated window setpoint increased, the heating load of radiant floor heating tended to decrease, and the heating load ratio was approximately 0.14% at 34 °C.

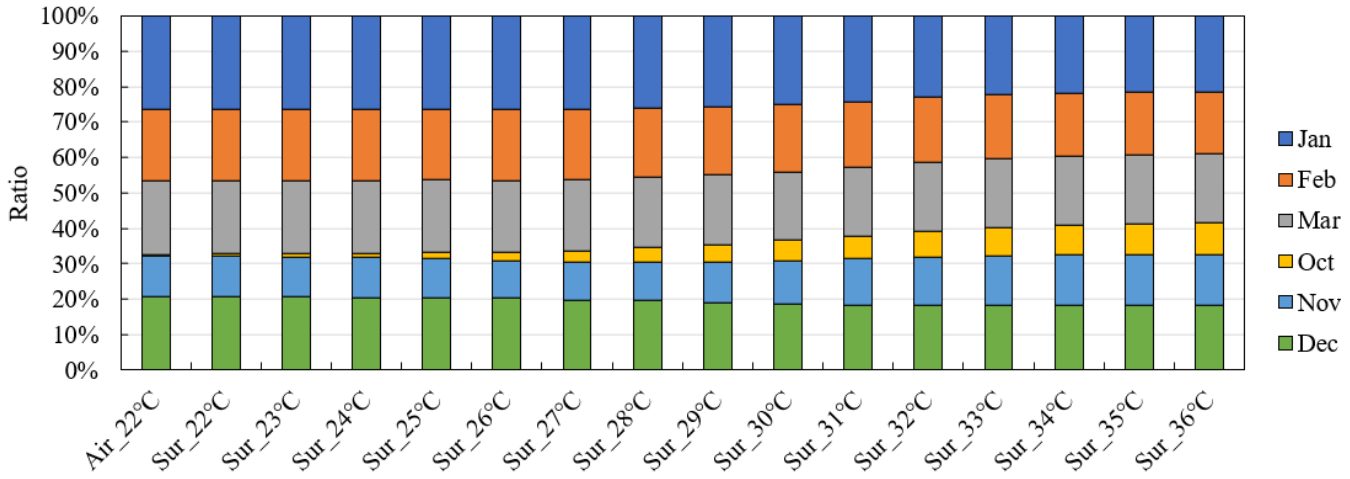

Figure 14. Ratio of monthly heating load to annual heating load.

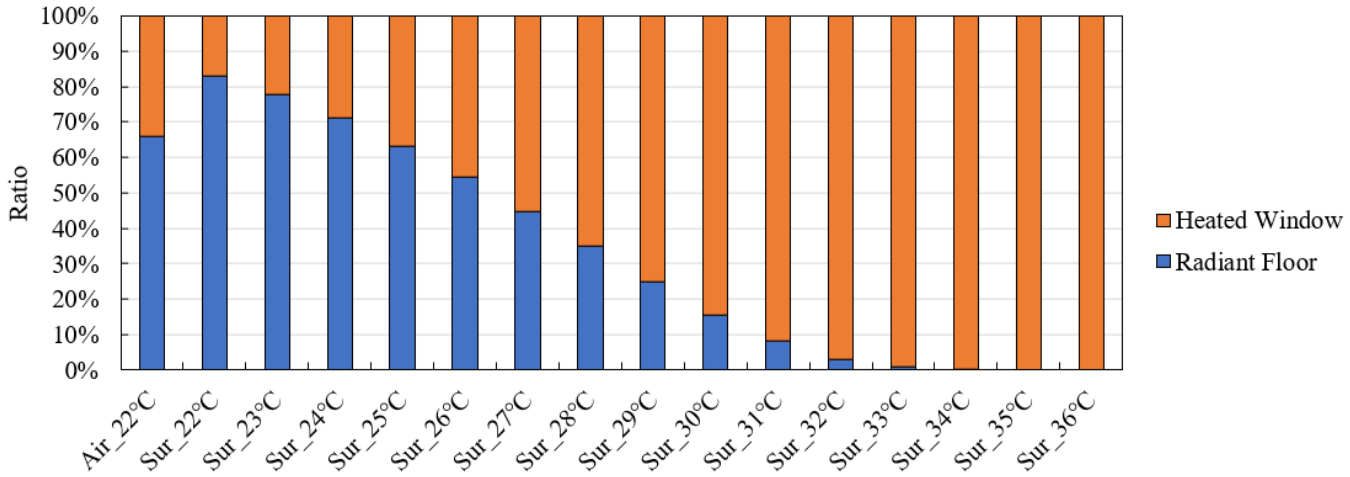

Figure 15. Ratio of heating load to annual heating load for each heating system.

The surface setpoint at which the heating load ratios to the heating systems' total heating load were the most similar to "Air_22 °C" was 25 °C; at this setting, the load ratios of floor heating and window heating were 63.26% and 36.74%, respectively. This was because the air temperature control method with a setpoint of 22 °C and the window surface temperature control method with a setpoint of 25 °C had a similar inner surface temperature of the heated window. Figure 16 presents the inner surface temperatures of the heated window in the air temperature control model with a setpoint of 22 °C and the surface temperature control model with setpoints of 22 °C, 25 °C, and 28 °C, from 1 to 14 December. During the daytime when the window temperature increased owing to irradiance, the same temperature was observed regardless of the control method and setpoint. During the nighttime, each model showed different inner surface temperatures of the heated window, and the model of the air temperature control and the model of the surface temperature control with a setpoint of 25 °C exhibited the most similar surface temperature trends.

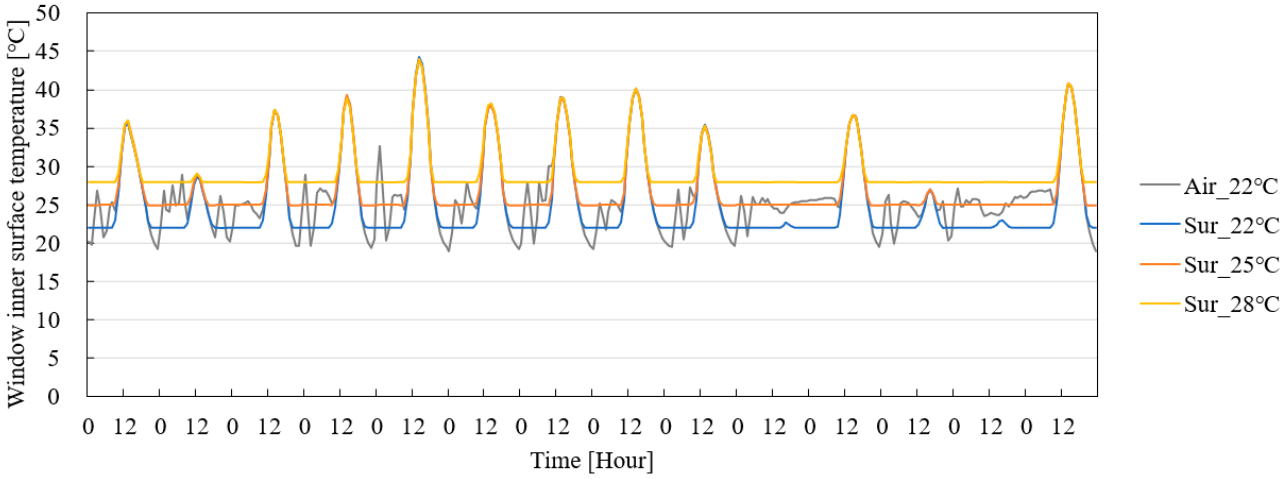

Figure 16. Inner surface temperature of the window.

4.2. Thermal Comfort Comparison According to Control Method and Setpoint

The thermal comfort of the hybrid heating models was analyzed. The thermal comfort in the glass and room zones was analyzed, and the ratio of the time for cumulative analysis for each PMV range to all periods was examined.

Figure 17 shows the thermal comfort analysis results in the glass zone of each model. As heated window heating was applied to the glass zone, the changes in the PMV were sensitive to the heated window setpoint. In the air temperature control model, the cumulative time for thermal comfort ($-0.5 \leq$ PMV ≤ 0.5) was 3036 h, approximately 69.51% of the total time (4368 h). The time for thermal comfort tended to decrease as the setpoint of the heating window increased, and it sharply decreased from a specific temperature.

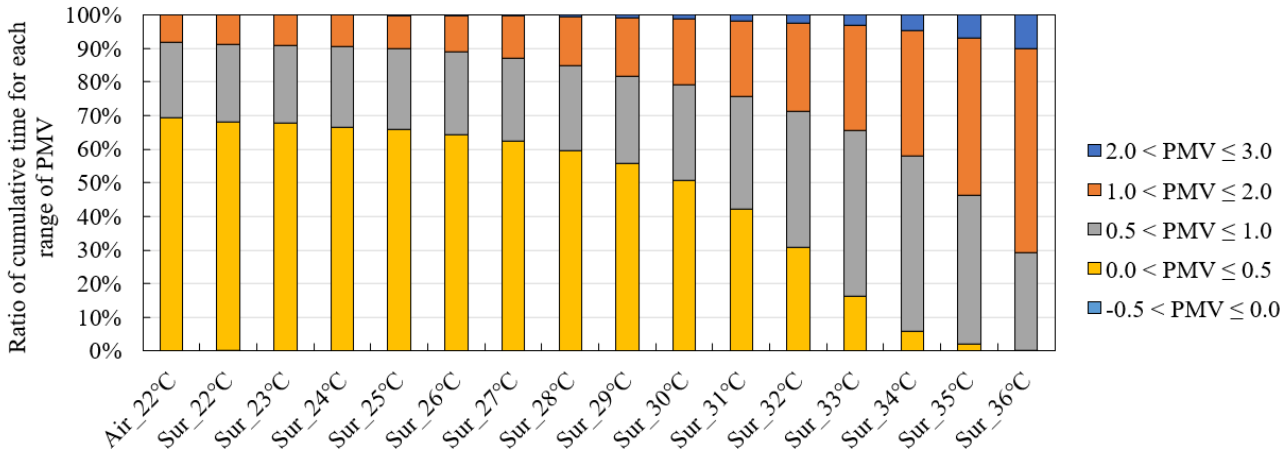

Figure 17. Ratio of cumulative time for each range of PMV for the glass zone.

Figure 18 presents the glass zone's air temperature and heated window inner surface temperature for the air temperature control model with a setpoint of 22 °C and the surface temperature control model with various setpoints. The figure shows the temperature distribution for one week from 1 to 7 December. The air temperature of the glass zone for the air temperature control model was similar to the air temperature control model with a surface setpoint of 22 °C and 25 °C. However, suppose that the surface setpoint is higher than 30 °C. In that case, the glass zone's air temperature for the surface temperature control model is higher than the air temperature control model during daytime and nighttime. It means that the air temperature is higher than the air setpoint of the room zone.

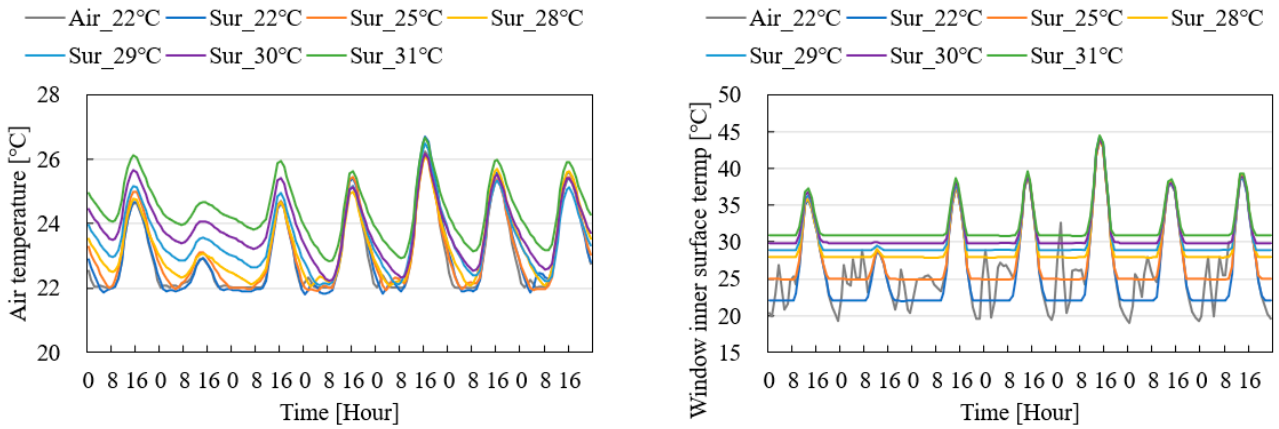

(**a**) (**b**)

Figure 18. Air temperature of the glass zone and the inner surface temperature of the window. (**a**) Air temperature of glass zone; (**b**) Window inner surface temperature.

Figure 19 shows the cumulative time ratio according to the thermal comfort range in the room zone. Overall, the cumulative time ratio of the thermal comfort range ($-0.5 \leq$ PMV ≤ 0.5) was higher than that of the glass zone. In the air temperature control method, the time for thermal comfort was 3492 h, approximately 79.95% of the total time. In contrast, the surface temperature control method with the same setpoint was about 3% lower, at 76.85%.

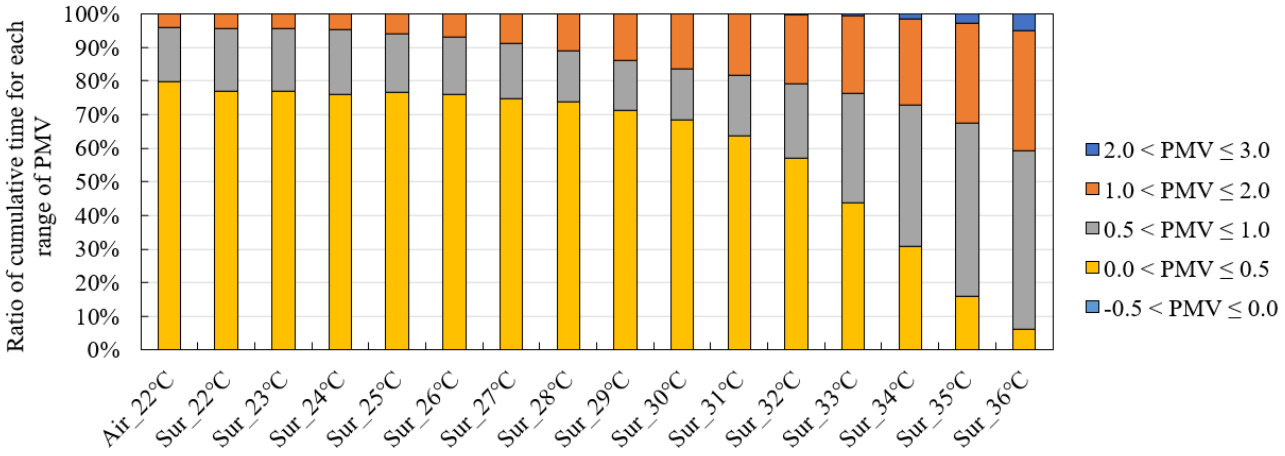

Figure 19. Ratio of cumulative time for each range of PMV for the room zone.

Figure 20 shows the combined annual cumulative heating load and the ratio of time for thermal comfort of the air temperature control and surface temperature control models. As analyzed above, when the surface setpoint was 30 °C, the heating load was the lowest at 1063.17 kWh. Therefore, a surface setpoint of 30 °C was found to be the most suitable for the heating load. In contrast, the time for thermal comfort was the highest in both the glass and room zones when the air setpoint was 22 °C. Table 9 summarizes the optimal setpoints and differences in the parameters according to the control method.

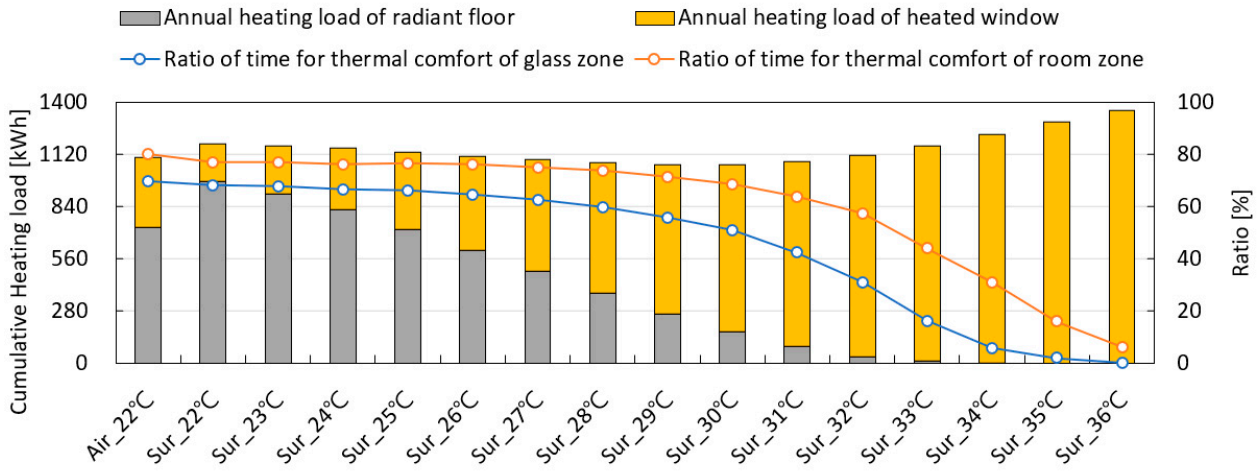

Figure 20. Annual heating load and ratio of time for thermal comfort.

Table 9. Setpoint, heating load, and thermal comfort for each control method.

		Optimal Setpoint (°C)	Annual Heating Load (kWh)	Ratio of Time for Thermal Comfort (%)	
				Glass Zone	Room Zone
Air temperature control		22	1101.96	69.51	79.95
Surface temperature control	Heating load	30	1063.17	50.80	68.59
	Thermal comfort	22	1174.65	68.22	76.85
	Optimal control	26	1109.26	64.4	76.08

In surface temperature control, the heating load of the model optimized for heating load was 9.05% lower than the model optimized for thermal comfort, and the ratio of time of the thermal comfort was also 25.54% and 10.75% lower in the glass zone and room zone, respectively. In contrast, for the model for thermal comfort, the heating load increased by approximately 10.49%, and the ratio of time for thermal comfort improved by 33.29% and 12.04% in the glass and room zones, respectively.

To propose the optimal surface setpoint by synthesizing the heating load and thermal comfort, it is necessary to find the surface setpoint that maximizes the decrease in heating load while minimizing the reduction in the ratio of the time of thermal comfort. Based on Figure 19, the setpoint can be estimated by comprehensively considering the heating load and thermal comfort. Up to a setpoint of 26 °C, the reduction in the ratio of time for thermal comfort in the glass zone and room zone was not large, and the heating load was improved.

5. Conclusions and Discussion

This study evaluated the effectiveness of the heated window heating system in a typical residential building in South Korea. This study compared the heating load and thermal comfort of three different heating system types (i.e., radiant floor, heated window, and hybrid heating systems) in the Gangneung location, South Korea. The surface temperature variations of the heated window were investigated to determine appropriate setpoint temperatures regarding indoor thermal comfort and energy consumption.

The compared results of heating loads for each heating system indicated that applying the heated window heating method decreased the peak and cumulative heating load. The window surface was heated by the heated window system, which caused an increase in the surface temperature of the glass. Theoretically, if the indoor surface temperature of the heated window system is higher than the indoor air temperature, the heat loss through the window is zero, which is advantageous regarding the heating load.

Compared to the heating load for radiant floor heating, the heating reductions were about 34.40% (ground floor: 3.73%, typical floor: 35.06%) and 59.05% (ground floor: 60.32%, typical floor: 57.79%) for the heated window and hybrid heating systems, respectively. In addition, the ratios of time for thermal comfort in the glass zone and room zone were 72.45% (ground floor: 74.77%, typical floor: 70.12%) for radiant floor heating, 81.54% (ground floor: 83.79%, typical floor: 79.29%) for heated window heating, and 77.51% (ground floor: 80.29%, typical floor: 74.73%) for hybrid heating.

Such results demonstrated that the heated window heating system could present better performance compared to the existing radiant floor heating method regarding the heating load and thermal comfort. However, because the floor surface temperature was lower under the heated window heating system than in the radiant floor heating system, the hybrid heating system is more suitable for residential household types in South Korea.

A suitable control method and setpoint were estimated by evaluating the heating load and thermal comfort according to the control method in the hybrid heating system. The annual heating load was the lowest when the heated window surface temperature was set to 30 °C. However, operating at a surface temperature of 30 °C caused the indoor space to overheat, which was disadvantageous in terms of indoor thermal comfort levels. In the case of the air temperature being set to 22 °C, the time ratio for the indoor thermal comfort increased when compared with the surface temperature control. However, by comprehensively considering the heating load and thermal comfort to estimate the control method and setpoint, the heating load and thermal comfort levels were enhanced when the heated window surface temperature was controlled to 26 °C.

This study has proved the effectiveness of the heated window systems as a building heating appliance. Although the thermal insulation performance of windows has substantially improved, the windows continue to be a thermally weak component of the building envelope. Heat loss and condensation occur in thermally inefficient windows, and cold drafts can affect the occupant's thermal comfort. Hence, adding a heating functionality to these windows should not only prevent condensation and improve thermal comfort, but can also make them applicable to indoor heating. It was confirmed that the control of the heated windows for the thermal comfort of occupants close to the heated windows could adversely affect the thermal comfort of occupants far from the heated windows. In addition, the optimal setpoint temperature for the thermal comfort and energy performance under the conditions of this study (i.e., type of building, the region and the climate, internal gain, thermal insulation performance of building element) was also proposed. However, since the building model and area for evaluation of usefulness was limited to one, additional research is needed to generalize the optimal setpoint temperature.

This study used a heating load to assess the effectiveness of heated windows as an index. The primary energy consumption and carbon emissions can vary according to the energy source of the heating system (electricity, gas, etc.). Furthermore, because this study only utilized simulation-based analysis, future work should include experimental analysis and evaluation through full-scale mock-ups and their application in a practical manner.

Author Contributions: Conceptualization, J.Y., D.K., H.L. and K.L.; methodology, H.L., K.L. and M.O.; software, H.L. and K.L.; validation, H.L. and K.L. and D.K.; formal analysis, H.L. and K.L.; investigation, H.L., K.L. and M.O.; resources, H.L. and K.L.; data curation, H.L., K.L. and E.K.; writing—original draft preparation, H.L. and K.L.; writing—review and editing, H.L. and D.K.; visualization, H.L. and K.L.; supervision, J.Y. and D.K.; project administration, J.Y. and D.K.; funding acquisition, J.Y. All authors have read and agreed to the published version of the manuscript.

Funding: This work is supported by the Korea Agency for Infrastructure Technology Advancemen (KAIA) grant funded by the Ministry of Land, Infrastructure and Transport (Grant 21CTAP-C163698-01).

Data Availability Statement: Not applicable.

Conflicts of Interest: The authors declare no conflict of interest.

References

1. UN Environment Programme, 2022 Global Status Report for Buildings and Construction. Available online: https://www.unep.org/resources/publication/2022-global-status-report-buildings-and-construction (accessed on 22 December 2022).
2. Lee, H.; Choi, M.; Lee, R.; Kim, D.; Yoon, J. Energy performance evaluation of a plus energy house based on operational data for two years: A case study of an all-electric plus energy house in Korea. *Energy Build.* **2021**, *252*, 111394. [CrossRef]
3. International PASSIVE HOUSE Association. Passive House Guidelines. Available online: https://passivehouse-international.org/index.php?page_id=80 (accessed on 22 December 2022).
4. Ihm, P.; Park, L.; Krarti, M.; Seo, D. Impact of window selection on the energy performance of residential buildings in South Korea. *Energy Policy* **2012**, *44*, 1–9. [CrossRef]
5. Myhren, J.A.; Holmberg, S. Flow patterns and thermal comfort in a room with panel, floor and wall heating. *Energy Build.* **2008**, *40*, 524–536. [CrossRef]
6. Moreau, A.; Sansregret, S.; Fournier, F. Modeling and study of the impacts of electrically heated windows on the energy needs of buildings. In Proceedings of the WSEAS International Conference on Heat Transfer, Thermal Engineering and Environment, Rhodes, Greece, 20–22 August 2008; pp. 76–83.
7. Werner, A.; Roos, A. Condensation tests on glass samples for energy efficient windows. *Sol. Energy Mater. Sol. Cells* **2007**, *91*, 609–615. [CrossRef]
8. Werner, A.; Roos, A. Simulations of coatings to avoid external condensation on low U-value windows. *Opt. Mater.* **2008**, *30*, 968–978. [CrossRef]
9. Kurnitski, J.; Jokisalo, J.; Palonen, J.; Jokiranta, K.; Seppänen, O. Efficiency of electrically heated windows. *Energy Build.* **2004**, *36*, 1003–1010. [CrossRef]
10. Lee, R.; Kang, E.; Lee, H.; Yoon, J. Heat flux and thermal characteristics of electrically heated windows: A case study. *Sustainability* **2022**, *14*, 481. [CrossRef]
11. Cakó, B.; Lovig, D.; Ózdi, A. Measuring the effects of heated windows on thermal comfort. *Pollack Periodica* **2021**, *16*, 114–119. [CrossRef]
12. Lee, D.-H.; Yoon, J.-H.; Lee, K.-W.; Seo, M.-G. Heating energy performance of heated glass according to insulation level of the residential building. *J. KSES* **2021**, *41*, 73–84. [CrossRef]
13. Lee, D.-H.; Yoon, J.-H.; Oh, M.-H. Analysis of temperature and total heat of heated glass through experimental measurement and three-dimensional steady-state heat transfer analysis. *KIEAE J.* **2015**, *15*, 111–116. [CrossRef]
14. Basok, B.; Davydenko, B.; Goncharuk, S.; Pavlenko, A.; Lysenko, O.; Novikov, V. Features of heat transfer through a window with electric heating. In Proceedings of the 2022 IEEE 8th International Conference on Energy Smart Systems (ESS), Kyiv, Ukraine, 12–14 October 2022; pp. 195–198. [CrossRef]
15. Krukovskyi, P.; Smolchenko, D.; Krukovskyi, G.; Deineko, A. Analysis of the heating capacity of electrically heated windows. *Thermophys. Therm. Power Eng.* **2021**, *43*, 62–67. [CrossRef]
16. Mitsui, A.; Sato, K. Thermal stability of electrical resistance of (ZnO:Ga,Y)/(ZnO:Ga)/(ZnO:Ga,Y) multilayers for electrically heated windows. *Vacuum* **2004**, *74*, 747–751. [CrossRef]
17. Rueegg, T.; Dorer, V.; Steinemann, U. Must cold air down draughts be compensated when using highly insulating windows? *Energy Build.* **2001**, *33*, 489–493. [CrossRef]
18. Wu, Q.; Wang, Z.; Dong, J.; Liu, J. A method for judging the overheating of the radiator in the compensation of window downdraught based on thermal image velocimetry. *Build. Environ.* **2021**, *197*, 107858. [CrossRef]
19. Kim, S.-J.; Choi, H.; Kim, K.-H.; Hong, Y.-J.; Hwang, I.-S.; Lee, D.-W.; Chun, S.-K. Heating Glass and Manufacturing Method Thereof. U.S. Patent 8916805B2, 12 December 2014.
20. Pilkington. NSG TEC Overview. Available online: https://www.pilkington.com/en/global/knowledge-base/types-of-glass/powered-by-nsg-tec/overview (accessed on 20 January 2023).
21. Pilkington. NSG TEC Technical Data Sheet. Available online: https://www.pilkington.com/ (accessed on 20 January 2023).
22. Perkin Elemer. Available online: https://www.perkinelmer.com/ (accessed on 22 December 2022).
23. *ISO 9050*; Glass in building—Determination of Light Transmittance, Solar Direct Transmittance, Total Solar Energy Transmittance, Ultraviolet Transmittance and Related Glazing Factor. International Organization for Standardization: Geneva, Switzerland, 2003.
24. *KS L 2514*; Testing Method on Transmittance and Emittance of Heat Glasses and Evaluation of Solar Heat Gain Coefficient. Korea Industrial Standards: Seoul, Republic of Korea, 2011.
25. International Commission on Illumination. CIE Standard Illuminant D65. Available online: https://cie.co.at/datatable/cie-standard-illuminant-d65 (accessed on 20 January 2023).
26. Energy System Research Unit of University of Strathclyde Glasgow. Available online: https://www.strath.ac.uk/research/energysystemsresearchunit/applications/esp-r/ (accessed on 22 December 2022).
27. The Center of Information for National Law. Available online: https://www.law.go.kr (accessed on 20 January 2023).
28. Korea Meteorological Administration. Available online: https://data.kma.go.kr/ (accessed on 22 December 2022).
29. Beck, H.; Zimmermann, N.; McVicar, T.; Vergopolan, N.; Berg, A.; Wood, E.F. Present and future Köppen-Geiger climate classification maps at 1 km resolution. *Sci. Data* **2018**, *5*, 180214. [CrossRef]
30. Fanger, P. *Thermal Comfort—Analysis and Applications in Environmental Engineering*; Danish Technical Press: Copenhagen, Denmark, 1982; pp. 128–133.

31. *ISO 7730:2005*; Ergonomics of the Thermal Environment—Analytical Determination and Interpretation of Thermal Comfort Using Calculation of the PMV and PPD Indices and Local Thermal Comfort Criteria. International Organization for Standardization: Geneva, Switzerland, 2005.
32. *Standard 55-2010*; Thermal Environmental Conditions for Human Occupancy. ANSI/ASHRAE: Peachtree Corners, GA, USA, 2010.

Disclaimer/Publisher's Note: The statements, opinions and data contained in all publications are solely those of the individual author(s) and contributor(s) and not of MDPI and/or the editor(s). MDPI and/or the editor(s) disclaim responsibility for any injury to people or property resulting from any ideas, methods, instructions or products referred to in the content.